Journal of Advances and Scholarly Researches in Allied Education
Vol. 16, Issue No. 6, May-2019, ISSN 2230-7540

Analysis of Generalized Lienard Oscillators

Goutam Pal[1]* Dr. Sonal Bharti[2]

[1] Research Scholar, Department of Mathematics, Sri Satya Sai University of Technology & Medical Sciences, Sehore, M.P.

[2] Research Guide, Department of Mathematics, Sri Satya Sai University of Technology & Medical Sciences, Sehore, M.P

Abstract – A systematic qualitative study of generalized Lienard oscillators is performed here proposed by C. [J.Math.Phys.56,012903 (2015)] Quesne. It also explores the influence of dissipation. We show that while the first potential admits a pair of equilibrium points, one of which is usually a centre for both signs of the coupling strength λ, the other points to a centre for λ < 0 but a saddle λ > 0 by performing a local analysis of the governing potentials. A significant finding is that in the presence of a periodic force term f cos ωt.

Key Words – Oscillation, Nonlinear, Liénard System, Differential Equations, Dynamic System

----------X----------

1.1 INTRODUCTION

► Dynamical System

Dynamics is the analysis of transition, and a dynamic system is just a recipe for telling how a system interacts and changes over time (state variables). It is possible to consider a dynamic system as an entity of some kind, the state of which evolves in time according to some dynamic law. The theory of dynamic systems provides a wide variety of analytical, geometrical, topological, and computational techniques for analyzing differential equations and iterated mappings.

It is possible to classify any system that changes over time as a dynamical system. More specifically, the system evolves over time in such a way that dynamical systems are called the states of the system at time t depend on the states of the system at earlier times. In other words, a dynamic system consists of a number of potential states along with a law that, in terms of past states, defines the present states ([1]). Variable dynamical systems may be categorized as a discrete dynamical system or as a continuous dynamical system according to the character of the time.

The time variable in discrete dynamical system is discrete i.e, $t \in \mathbb{Z}$ *or* $\mathbb{N}$ or N and the evolution is determined by a difference equation. For example $x_{t+1} = f(x_t, x_{t-1}, .., x_{t-n})$; $t \in \mathbb{Z}$ *or* $\mathbb{N}$ is the form of a discrete dynamical system. A continuous dynamical system is represented by a differential equation

$$\dot{x} = f(x,t), x \in U \subseteq \mathbb{R}^n, t \in \mathbb{R} \quad \text{.....(1.1.1)}$$

possessing a unique solution $x(t,t_0) = x(t)$ satisfying the condition $x(t0) = x_0$.

A flow is a deterministic continuous system on a manifold which is continuously differentiable with respect to time. In general a complete flow $\phi_t(x)$ is a one parameter, differentiable mapping $\phi : \mathbb{R} \times M \to M$, such that

(a) $\phi_0(x) = x$ and

(b) for all t and $s \in \mathbb{R}$,

$\phi_t \circ \phi_s = \phi_{t+s}$ where M is the manifold of phase space for a dynamical system and the composition symbol o means $\phi_t \circ \phi_s(x) = \phi_t(\phi_s(x))$.

Example: Lorenz system, $x = \sigma(y - x)$, $y = rx - y - xz$, $z = xy - bz$, where σ, r, b >0 represent a continuous dynamical system.

► Chaos

There is an enormous obsession with uncertainty today. The science of surprises, the non-linear and the unexpected, is chaos. This instructs us to expect the unexpected. While most traditional science deals with supposedly predictable phenomena such as gravity, electricity or chemical

reactions, Chaos theory deals with nonlinear things such as turbulence, weather, the stock market, our brain states, and so on, that are effectively impossible to predict or regulate. If it has the following properties, a dynamic system is said to be chaotic [1].:

1) Initial situations must be sensitive to it. Sensitivity to initial conditions implies that other points with substantially different future paths or trajectories are arbitrarily closely approximated by each point in a chaotic system. An arbitrary minor change or disruption of the current trajectory may then lead to dramatically different future behaviour. A consequence of sensitivity to initial conditions is that the system is no longer predictable if we start with only a finite amount of knowledge about the system after a certain time. In the case of weather that is normally only predictable about a week ahead, this is most familiar.

2) It must be transitive topologically. Topological transitivity or topological mixing means that the system evolves over time such that its phase space ultimately overlaps with any other given region in any given region or open set. Such a complex structure can therefore not be broken down into two disjoint sets of non-empty interiors that do not interact under the transition.

3) Its periodic orbit must be dense. Dense periodic orbit means that arbitrary close to every point there is a periodic orbit in the phase space.

1.2 QUALITATIVE ANALYSIS OF QUADRATIC LIENARD EQUATION

Nonlinear autonomous differential equations of second order have proved to be of much interest in the investigation of dynamical systems and nonlinear analysis [2-9].

$$\ddot{x}+r(x)\dot{x}^2+x(x)=0 \quad \ldots\ldots\ldots\ldots\ldots (1.2.1)$$

which is a to quadratic Lienard class.

where an overdot indicates a derivative with respect to the time variable t and *r(x)* and s(x) are two continuously differentiable functions of the spatial coordinate x. The following specific forms of r and s which are odd functions of x, namely

$$r(x)=-\frac{\lambda x}{1+\lambda x^2}, g(x)=\frac{\alpha^2 x}{1+\lambda x^2}, \lambda>0 \quad \ldots\ldots\ldots\ldots\ldots (1.2.2)$$

where *α* and *λ* are nonzero real numbers, lead to a nonlinear equation defined by

$$\left(1+\lambda x^2\right)\ddot{x}-\lambda x\dot{x}^2+\alpha^2 x=0 \quad \ldots\ldots\ldots (1.2.3)$$

The Lagrangian relevant to (1.2.3)

$$L=\frac{1}{2}\frac{1}{1+\lambda x^2}\left(\dot{x}^2-\alpha^2 x^2\right) \quad \ldots\ldots\ldots\ldots (1.2.4)$$

was studied by Mathews and Lakshmanan (ML) [8] long time ago in the search of a one-dimensional analogue of some quantum field theoretic model. One can observe that (2.4) speaks of a A-dependent deformation of the standard harmonic oscillator Lagrangian. Carmena et al [10] also pointed out that the kinetic term in this Lagrangian is invariant under the tangent lift of the vector field $X_x(\lambda)=\sqrt{1+\lambda x^2}\frac{\partial}{\partial x}$.

The corresponding Hamiltonian represents a position-dependent effective mass system guided by the mass function of the specific type $m(x)=\frac{1}{1+\lambda x^2}$. In the literature dynamics of several types of nonlinear systems have been found to be influenced by a position-dependent effective mass [11-13]. From a physical point of view problems of position-dependent effective mass have relevance in describing the flow of electrons in problems of compositionally graded crystal, quantum dots and liquid crystals [14-17].

As is well known the nonlinear dynamics described by (1.2.3) admits, in particular, a periodic solution for x(t) given by the simple harmonic form

$$x(t)=A\sin(\omega t+\phi) \quad \ldots\ldots\ldots\ldots\ldots (1.2.5)$$

but with the restriction that the frequency ω is related to the amplitude A by the constraint $\omega^2=\frac{\alpha^2}{1+\lambda A^2}$. The amplitude thus depends on the frequency.

From the form of the Lagrangian (1.2.4) it is easy to identify the corresponding potential V (x) as given by

$$V(x)=\frac{1}{2}\frac{\alpha^2 x^2}{1+\lambda x^2} \quad \ldots\ldots\ldots\ldots\ldots (1.2.6)$$

Recently Quesne [18] extended the above potential to two different types of generalizations by introducing a two-parameter deformation of the harmonic oscillator potential by bringing in an additional phenomenological parameter β in the manner:

(a) $$V_1=\frac{1}{2}\frac{\alpha^2 x^2-2\beta x}{1+\lambda x^2} \quad \ldots\ldots\ldots (1.2.7)$$

(b) $$V_{11}=\frac{1}{2}\frac{\alpha_2 x^2-2\beta x\left(1+\lambda x^2\right)}{1+\lambda x^2} \quad \text{.....(1.2.8)}$$

while keeping the kinetic part of (1.2.4) unchanged. The respective Euler-Lagrange equations that follow from (1.2.7) and (1.2.8) read

$$\left(1+\lambda x^2\right)\ddot{x}-\lambda x\dot{x}^2+\alpha^2 x-\beta\left(1-\lambda x^2\right)=0 \quad \text{.....(1.2.9)}$$

$$\left(1+\lambda x^2\right)\ddot{x}-\lambda x\dot{x}^2+\alpha^2 x-\beta\sqrt{\left(1-\lambda x^2\right)}=0 \quad \text{.....(1.2.10)}$$

Let us emphasize that the functional form corresponding to s(x) in the above equations is not odd but of a mixed type consisting of a term that is odd and a term that is even. With an extra parameter ft at hand, quite expectedly, the potentials V_1 and V_{11} allow dealing with richer behavior patterns of the solutions of the corresponding Euler-Lagrange equations than the ones provided by (4) for the ML case. One of the guiding factors in this regard is the sign of the deformation parameter λ that corresponds to different asymptotic behavior of the two potentials V_1 and V_{11} and the locations of the minimum for the latter. The first integral of the Euler-Lagrange equation when suitably confronted with the integration constant and the underlying discriminant also give crucial restrictions on the domains of the energy of the system for a physically viable solution.

In this paper, we interpret the generalized nonlinear oscillators that are guided by V_1 and V_{11} as examples of dynamical systems and perform a qualitative analysis to determine some interesting local properties for them. We also take up the issue of chaos in the presence of a periodic force term $f\cos\omega t$ for both the systems by fine-tuning some of the coupling parameters.

1.3 ANALYSIS OF THE POTENTIAL V/(X) AND V_{11}(X)

► Analysis of the Potential V/(x)

Let us rewrite the Euler-Lagrange equation in the presence of Vj as the following system of coupled equations

$$\dot{x}=y$$
$$\dot{y}=\frac{\lambda xy^2}{1+\lambda x^2}-\frac{\alpha^2 x}{1+\lambda x^2}+\frac{\beta\left(1-\lambda x^2\right)}{1+\lambda x^2} \quad \text{.....(1.3.1)}$$

The resulting fixed points are readily identified to be located at the points (x^*_1,0) and (x^*_2, 0) where

$$x^*_{1,2}=\left(-\alpha^2\pm\sqrt{\alpha^2+4\lambda\beta^2}\right)/2\lambda\beta \quad \text{.....(1.3.2)}$$

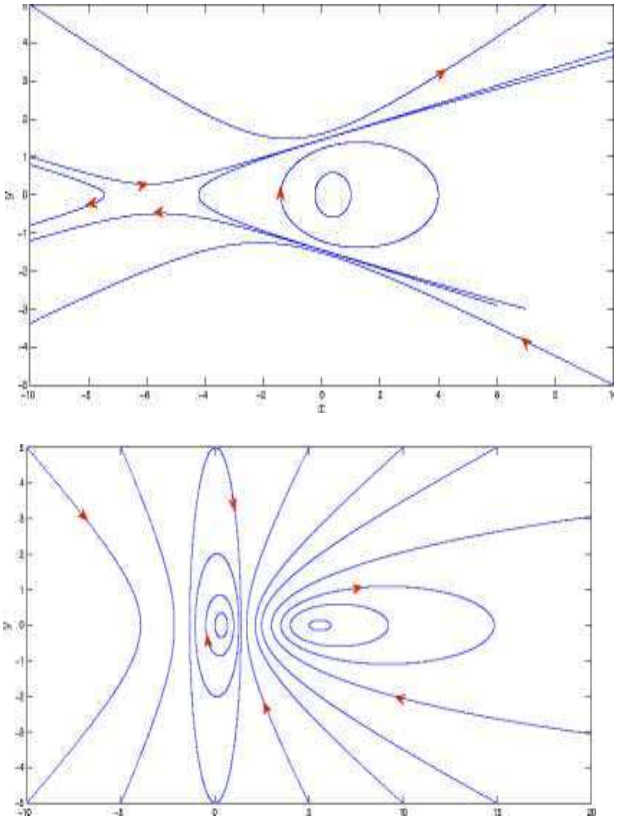

Figure 1.1: Phase diagram of the system (2.11) for (a) λ = 0.5, (b) λ = -0.5 with β = 0.34, *a* = 1.0.

The positivity of the discriminant leads to the restriction $\lambda>-\alpha^4/4\beta^2$. Evaluating the Jacobian matrix at the fixed points we obtain

$$J\big|_{(x_{1,2},0)}=\begin{pmatrix}0 & 1\\ A_{21} & 0\end{pmatrix} \quad \text{.....(1.3.2)}$$

Where

$$A_{21}=\left(-\alpha^2+\lambda\alpha^2x_c^2-4\lambda/\beta x_c\right)/\left(1+\lambda x_c^2\right)^2 \text{ and } x_c=x^*_{1,2} \quad \text{.....(1.3.3)}$$

For λ > 0, the respective eigenvalues of J at x_1* and x_2* are

$$\pm i\sqrt{\frac{2\lambda\beta^2}{\sqrt{D}-\alpha^2}},\pm\sqrt{\frac{2\lambda\beta^2}{\sqrt{D}+\alpha^2}} \quad \text{.....(1.3.4)}$$

where $D=\alpha^4+4\beta^2\lambda>0$ implying $\sqrt{D}>\alpha^2$. We therefore conclude that the point $(x_1^*, 0)$ is a center while the other one, namely $(x_2^*, 0)$, is a saddle point. The phase diagram of the system (2.11) is plotted in Figure 2.1a taking the parameter values $\lambda=0.5$, $\beta=0.34$ $\alpha=1.0$.

In case of λ < 0 the two eigenvalues of the Jacobian matrix (2.13) at x_1* and x_2*) are given by

$$\pm i\sqrt{\frac{-2\lambda\beta^2}{\alpha^2-\sqrt{D}}},\ \pm i\sqrt{\frac{-2\lambda\beta^2}{\alpha^2+\sqrt{D}}} \quad \text{.....(1.3.5)}$$

Where

$$D=\alpha^4+4\beta^2\lambda>0.\ \alpha^2>\sqrt{D}\ as\ -\alpha^4/4\beta^2\le\lambda<0$$

Here too the equilibrium points $(x_1^*, 0)$ and $(x_2^*, 0)$ correspond to centers since the eigenvalues of the Jacobian matrix are purely imaginary conjugate pairs for $\lambda < 0$. Figure 2.1b represents the phase portrait of the system (2.11) for $\lambda = -0.5$, $\beta = 0.34$ $\alpha = 1.0$.

These Figure 1.2a and Figure 1.2b are consistent with the linear analysis results.

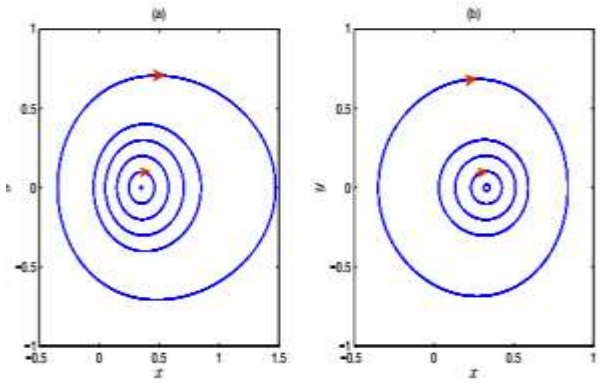

Figure 1.2: Phase portrait of the system (2.17) for (a) λ = 0.5 ,(b) λ = -0.5 ; with β = 0.34 , α = 1.0 .

► **Analysis of the Potential V_{11}(x)**

The dynamical system for the potential V_{11} (x) is described by the following set of equations

$$\dot{x}=y$$
$$\dot{y}=\frac{\lambda xy^2}{1+\lambda x^2}-\frac{\alpha^2 x}{1+\lambda x^2}+\frac{\beta\sqrt{1+\lambda x^2}}{1+\lambda x^2} \quad \text{.....(1.3.6)}$$

The two equilibrium points correspond to (x_1^*, 0) and (x_2^*, 0) where

$$x_{1,2}^*=\pm\frac{\beta}{\sqrt{\alpha^4-\lambda\beta^2}} \quad \text{.....(1.3.7)}$$

subject to the positivity condition. At the equilibrium points the Jacobian matrix takes the form

$$J\big|_{(x_{1,2},0)}=\begin{pmatrix}0 & 1\\ A_{21} & 0\end{pmatrix} \quad \text{.....(1.3.8)}$$

Where A_{21} is given by

$$A_{21}=\frac{\alpha^2\left(\lambda x_c^2-1\right)-\lambda\beta x_c\sqrt{1+\lambda x_c^2}}{\left(1+\lambda x_c^2\right)^2} \quad \text{.....(1.3.9)}$$

and x_c stands for $x_c = x_{1,2}^*$.

The eigenvalues of *J* represent a pair of degenerate conjugate complex quantities namely,

$$\pm\frac{i\left(\alpha^4-\lambda\beta^2\right)}{\alpha^3},\pm\frac{i\left(\alpha^4-\lambda\beta^2\right)}{\alpha^3} \quad \text{.....(1.3.10)}$$

While the linear stability analysis indicates the nonhyperbolic nature of the fixed points, as is well known such tests are not always in conformity with the nonlinear analysis. Indeed, the numerical simulation of the nonlinear system of 2.17, as shown in Figure 1.2, confirms that the linear stability results correctly predict the behavior of one of the equilibrium points namely x_1^* but it fails in the case of the other equilibrium point, x_2^*.

1.4 INFLUENCE OF AN EXTERNAL PERIODIC FORCING TERM

It is of considerable interest to study the dynamics of systems (1.4.1) and (1.4.2), under the influence of the external periodic forcing in the presence of additional damping, so that the respective equation of motion become

$$\left(1+\lambda x^2\right)\ddot{x}-\lambda x\dot{x}^2+\alpha^2 x-\beta\left(1-\lambda x^2\right)+\gamma\dot{x}=f\cos(\omega t) \quad \text{.....(1.4.1)}$$

$$and\ \left(1+\lambda x^2\right)\ddot{x}-\lambda x\dot{x}^2+\alpha^2 x-\beta\sqrt{\left(1+\lambda x^2\right)}+\gamma\dot{x}=f\cos(\omega t) \quad \text{.....(1.4.2)}$$

The above nonautonomous systems can be rewritten as the following three dimensional autonomous nonlinear dynamical systems respectively.

$$\dot{x}=y$$
$$\dot{y}=\frac{\lambda xy^2-\gamma y}{1+\lambda x^2}-\frac{\alpha^2 x}{1+\lambda x^2}+\frac{\beta\left(1-\lambda x^2\right)}{1+\lambda x^2}+\frac{f\cos z}{1+\lambda x^2} \quad \text{.....(1.4.3)}$$
$$\dot{z}=\omega$$

And

$$\dot{x}=y$$
$$\dot{y}=\frac{\lambda xy^2-\gamma y}{1+\lambda x^2}-\frac{\alpha^2 x}{1+\lambda x^2}+\frac{\sqrt{\beta\left(1+\lambda x^2\right)}}{1+\lambda x^2}+\frac{f\cos z}{1+\lambda x^2} \quad \text{.....(1.4.4)}$$
$$\dot{z}=\omega$$

We have done numerical simulations of the system (1.4.3) only. The results of simulation of the system (1.4.4) are qualitatively similar and hence not discussed.

1.5 RESULTS AND DISCUSSION

► Case-I: No Dissipation ($\gamma = 0$)

We start with the dynamics of the ML-model in the absence of dissipation. Thus we set $\gamma = 0$ and consider a set of sample parameter values $\lambda = -0.5$, $\alpha = 2.0$, $\gamma = 0.0$, w = 1.0 , $f = 5.0$ to plot the phase portrait in the xy-plane. It reveals the quasi-periodic nature of the system whose character survives for a wide range of inputs for the external periodic forcing term.

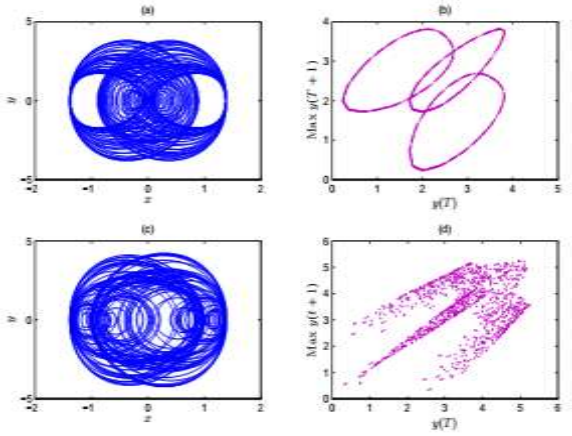

Figure 1.3: Phase portrait of the system (1.4.4) with $\lambda = -0.5$, $\alpha = 2.0$, $\gamma = 0.0$, $\omega = 1.0$, f=5.0 for different value of β (a) $\beta = 0.001$, (c) $\beta = 0.1$; (b) and (d) represent corresponding Poincaré return map.

The phase diagram in the system's xy plane (2.24) was plotted in Figure 1.3 for the parameter $\lambda = -0.5$, $\alpha = 2.0$, $\gamma = 0.0$, $\omega = 1.0$, f = 5.0 corresponding to the test values of f = 5.0 as given by $\beta = 0.001$ and $\beta = 0.1$. These β values represent small and moderate deviations from the ML-model. The case of $\beta = 0.001$ is shown in Figure 1.3a, while the first return map of Poincare is shown in Figure 1.3b. We note that on 3 smooth closed curves, the first return map data confirms the presence of the system's quasi-periodic behaviour. In Figure 1.3c, the phase diagram for $\beta = 0.001$ keeping the other parameters fixed is shown. The first return map, as shown in Figure 1.3d, shows a dramatic shift, however. In the above figure, the irregular scattering of points points to the presence of disorder in the system. Therefore, as shown by the transformation from quasi-periodicity to chaos, we note the sensitivity of the system (1.4.4) to the choice of the x-values as the value of x is modified from $\beta = 0.001$ by two orders of magnitude.

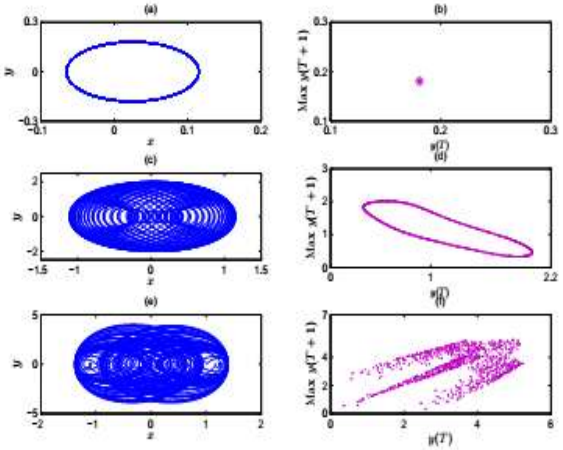

Figure 1.4: Phase portrait of the system (2.24) with $\lambda = -0.5$, $\alpha = 2.0$, $\beta = 0.1$, $\gamma = 0.0$, $\omega = 1.0$ for different value of f (a) f=0.0, (c) f=3.0, (e) f=5.0; (b), (d) and (f) represent corresponding poincaré return map.

Next, the phase diagrams and those for Poincar'e return maps for various values of forcing amplitude f are discussed for the system (2.24) for the data set $\lambda = -0.5$, $\alpha = 2.0$, $\beta = 0.1$, $\gamma = 0.0$, $\omega = 1.0$. In Figure 1.4, these are summarised.

We have plotted the phase portrait for f = 0.0 in Figure 1.4a and the corresponding first return map for Poincare is shown in Figure 1.4b. In the absence of any external forcing, the presence of just one point in Figure 1.4b proves the existence of a periodic orbit. The phase diagram of the system is presented in Figure 1.4c for f = 3.0 and the corresponding first return map of Poincare is shown in Figure 1.4d. The return map data is located on smooth closed curves and thus supports the system's quasi-periodic behaviour for f = 3.0.0. In Figure 1.5e, we have plotted the phase portrait for f = 5.0 and the corresponding return map information is plotted in Figure 2.4f. The abnormal set of points in the entire plane ensures the presence of chaos for f = 5.0. in the method. As in the previous case, therefore, the increase of the forcing amplitude also generates chaotic motion via the quasi-periodic path.

► Case-II: Dissipative Case ($\gamma \neq 0$)

Now, we turn to the inclusion in the model of the dissipation effects (2.24). The following fixed sample values of $\lambda = -0.5$, $\alpha = 2.0$, $\beta = 0.1$, $\omega = 1.0$ and $f = 5.0$ are retained towards this end and the dissipation parameter varies. An assorted set of values ranging from very small to fairly large values is considered for 7. In Figure 1.5a, we represent the phase portrait of 7 = 0.002 in the xy plane and the corresponding Poincare return map in Figure 1.5b. We find a collection of randomly distributed points that inform us about the system's chaotic character (2.24). Next to $\gamma = 0.02$, from the

machine phase portrait (2.24) shown in Figure 1.5c and the corresponding Poincare map in Figure 1.5d, a finite number of closed curves supporting the presence of quasi-periodic oscillations are noted. The phase portrait and time evolution of the variable y is shown in figures 1.5e and 1.5f for an order of magnitude higher value of γ = 0.1. The time evolution of the corresponding phase portrait of Figure 1.5f ensures that a periodic behaviour is present for = 0.1. The bifurcation diagram of the variable y is given in Figure 1.6 in relation to parameter 7. It is evident that the system needs to undergo a transformation from chaos to quasi periodicity with the increase of dissipation, and then settles to a periodic behaviour.

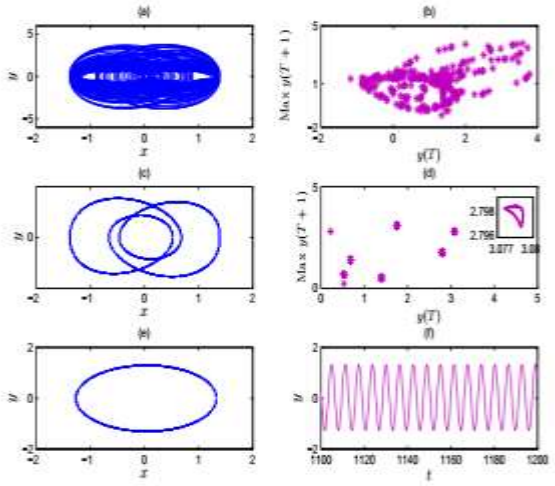

Figure 1.5: Phase portrait of the system (2.24) with λ = –0.5, a = 2.0, = 0.1, β = 1.0, ω=1.0 and f = 5.0 for different value of γ(a) γ = 0.002, (c) γ = 0.02, (e) γ = 0.1; (b), (d) represent corresponding poincare return map; (f) corresponding time series.

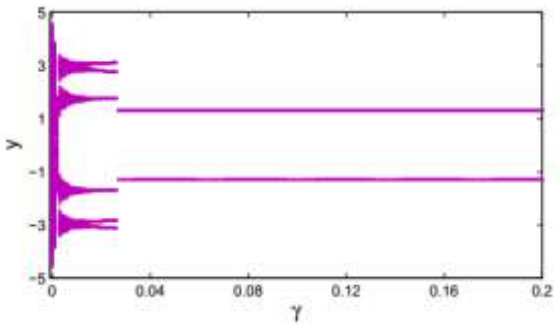

Figure 1.6: Bifurcation diagram of y with respect to parameter 7 of the system (2.24) with λ = –0.5, *a* = 2.0, β = 0.1, ω = 1.0 and *f* = 5.0.

1.6 CONCLUSION

In this chapter we studied the dynamical behavior of two quadratic schemes of generalized oscillators recently proposed by Quesne. We performed a local analysis of the governing potentials to demonstrate that while the first potential admits a typically center-like equilibrium point for both signs of the coupling strength λ, the second potential only admits to a center for λ < 0 but a saddle λ > 0. The second potential however reveals, from a linear stability analysis, only a center for both the signs of A. We have extended Quesne's scheme to include the effects of a linear dissipative term and shown how inclusion of an external periodic force term changes the qualitative behavior of the underlying systems drastically leading to the onset of chaos.

REFERENCES

[1] D. R. Nicholson (1981). Oscillating two-stream instability with pump of finite extent, Phys. Fluids, 24, 908.[43]

[2] A. C.L. Chian (1990). Nonthermal Radiation Processes in Interplanetary Plasmas, Revista Mexicana de Astronomia y Astrofisica, 21 (SI), pp. 541.

[3] A. C.L. Chian (1991). Electromagnetic radiation emitted by supersonic Langmuir turbulence in active experiments in space, Planetary and Space Sci., 39, pp. 1217.

[4] V. E. Zakharov (1972). Collapse of Langmuir Waves, Sov. Phys. JETP, 35, pp. 908.

[5] G. D. Doolen, D. F. DuBois, and H. A. Rose (1985). Nucleation of cavitons in strong langmuir turbulence, Phys. Rev. Lett., 54, pp. 804.

[6] H. T. Moon (1990). Homoclinic crossings and pattern selection, Phys. Rev. Lett., 64, pp. 412.

[7] X. T. He and C. Y. Zheng (1995). Spatiotemporal Chaos in The Regime of the Conserved Zakharov Equations , Phys. Rev. Lett., 74, pp. 78.

[8] S. E. Gibson, D. L. Newman, and M. V. Goldman (1995). Langmuir turbulence and three-wave nonlinear dynamics , Phys. Rev. E, 52, pp. 558.

[9] G. I. de Oliveira, L. P. L. de Oliveira, and F. B. Rizzato (1996). Low-dimensional phase-locked states in the Zakharov equations , Phys. Rev. E, 54, pp. 3239.

[10] G. I. de Oliveira, F. B. Rizzato, and A. C.L. Chian (1995). Length scale, quasiperi¬odicity, resonances, separatrix crossings, and chaos in the weakly relativistic Zakharov equations , Phys. Rev. E, 52, pp. 2025.

[11] Haas (2007). Variational approach for the quantum Zakharov system, Phys. Plas¬mas, 14, 042309.

[12] R. P. Sharma, K. Batra, and A. D. Verga (2005). Nonlinear evolution of the modu-lational instability and chaos using one-dimensional Zakharov equations and a simplified model , Phys. Plasmas, 12, pp. 022311.

[13] K. Batra, R. P. Sharma, and A. D. Verga (2006). Stability analysis of nonlinear evolution patterns of modulational instability and chaos using one-dimensional Zakharov equations, J. Plasma Phys., 72, pp. 671.

[14] T. Tajima and T. Taniuti (1990). Non-linear interaction of photons and phonons in electron-positron plasmas , Phys. Rev. A, 42, pp.3587.

[15] S. Eliezer and A. Ludmirsky (1983). Double layer (DL) formation in laser-produced plasma , Laser Part. Beams, 1, pp. 251.

[16] P. K. Shukla, M. Y. Yu, and N. L. Tsintsade (1984). Intense solitary laser pulse propagation in a plasma , Phys. Fluids, 27, pp. 327.

[17] M. D. Feit, A. M. Komashko, S. L. Musher, A. M. Rubenchik, and S. K. Turitsyn (1998). Electron cavitation and relativistic self-focusing in underdense plasma , Phys. Rev. E, 57, pp. 7122.

Corresponding Author

Goutam Pal*

Research Scholar, Department of Mathematics, Sri Satya Sai University of Technology & Medical Sciences, Sehore, M.P.